

Control Strategy of Solar Photovoltaic Generators with MPPT and Battery Storage in Micro Grid

Mr. G. Joga Rao¹, Dr. S.K. Shrivastava², Dr. D.K.Mangal³

¹ Research Scholar EEE Department, S.R. University , Alwar, Rajasthan, India

^{2,3} EEE Department, S.R. University , Alwar, Rajasthan, India

ABSTRACT

Maximum power point tracking (MPPT) of a photo voltaic system with different temperature and insolation conditions used for Micro grids can be explained in this paper. The micro grid conception permits small distributed energy resources (DERs) to act during a coordinated manner to produce a necessary quantity of active power and supportive service once needed. This paper proposes an approach of coordinated and integrated management of solar PV generators with the most power point following (MPPT) management and battery storage management to produce voltage and frequency (V-f) support to an islanded small grid. Also, active and nonnative/reactive power (P-Q) management with star PV, MPPT and battery storage is projected for the grid connected mode. The management ways show effective coordination between electrical converter V-f (or P-Q) management, MPPT management, and energy storage charging and discharging management. The penetration of PV systems as distributed generators in low-voltage grids has also seen significant attention. In addition, the need for higher overall grid efficiency and reliability has boosted the interest in the - concept. High-efficiency PV-based micro-grids require maximum power point tracking (MPPT) controllers to maximize the harvested energy due to the nonlinearity in PV module characteristics. The paper additionally shows a good coordination among taking part small resources whereas considering the case of fixing irradiance and battery state of charge (SOC) constraint. The simulation studies area unit dispensed with the IEEE 13-bus feeder check system in grid connected and islanded small grid modes. The results clearly verify the effectiveness of projected management strategies. The MPPT of a Photovoltaic System for Micro Grid operation is successfully designed and simulated by using MATLAB/Simulink Software in this paper.

Keywords: Photovoltaic (PV) System, Maximum Power Point Tracking (MPPT), Maximum Power Point(MPP), Incremental Active and Reactive Power management, Distributed Energy Resource (DER), Distributed Generation (DG), Voltage and Frequency Control.

I. INTRODUCTION

The traditional power systems comprise of the generation system which consists of large central power stations, the transmission and sub-transmission systems to deliver power from remote generating plants to the site near load centers, and the distribution system to serve all end users such as residential, commercial and industrial loads. The power flow is hence, unidirectional, that is, from generation to the load centers. With the ever increasing demand of electricity that has been raising important power system operational issues like voltage and frequency instability, the integration of distributed energy resources into the modern power systems have become

very popular since last few decades. The fast depletion of fossil fuel reserves and environmental concerns have provided greater incentive to integrate renewable energy based DERs like solar, wind and biomass in modern power systems. Renewable energy is currently widely used. One of these resources is solar energy. The photovoltaic (PV) array normally uses a maximum power point tracking (MPPT) technique to continuously deliver the highest power to the load when there are variations in irradiation and temperature. Renewable or non-conventional electricity generators employed in DG systems or Micro grids are known as distributed energy resources (DERs) or micro sources. The micro grid is a collection of distributed generators or micro resources,

energy storage devices, and loads which operate as a single and independent controllable system capable of providing both power and heat to the area of service. In a micro grid, the micro sources and storage devices are connected to the feeders through the Micro source controllers (MCs) and the coordination among the micro sources is carried out by the central controller (CC). The micro grid is connected to the medium voltage level utility grid at the point of common coupling (PCC) through the circuit breakers. When a micro grid is connected to the grid, the operational control of voltage and frequency is done entirely by the grid; however, a micro grid still supplies the critical loads at PCC, thus, acting as a PQ bus. In islanded condition, a micro grid has to operate on its own, independent of the grid, to control the voltage and frequency of the micro grid and hence, acts like a PV (power-voltage) bus. The operation and management in both the modes is controlled and coordinated with the help of micro source controllers (MCs) at the local level and central controller (CCs) at the global level. Similar to the traditional synchronous generator frequency control, the micro grid voltage and frequency control can also be performed using droop control methods. This paper proposes several control algorithms through which the capability of PV generators for voltage and frequency (V-f) control and active and nonnative/reactive power (P-Q) control in islanded and grid connected micro grids could be harnessed. The major contribution and novelty of the proposed control methods lie in the coordination among individual proposed control methods: MPPT control at the PV side, battery control, and V-f/P-Q control algorithm at the inverter side. These three control algorithms at three stages are jointly linked through a power balance objective at the DC and AC side of the inverter so that the DC side voltage is indirectly controlled at the desired value in order to maintain the AC side voltage at the utility desired voltage. Also, the proposed control methods have the capability of Handling battery state of charge (SOC) constraints through the coordination of controls between participating micro resources in the micro grid. This is a very important contribution from this work as compared to other literatures in this area. At the same time, the controls can seamlessly transform from one mode e.g., inverter P-Q control in grid connected mode to V-f control in islanded mode. The proposed control methods are validated with satisfactory results.

II. METHODS AND MATERIAL

1. Modeling of PV Cell

The model of the solar PV cell can be realized by an equivalent circuit that consists of a current source in parallel with a diode as shown in figure. 1 for ideal model R_s , R_p and C components can be neglected

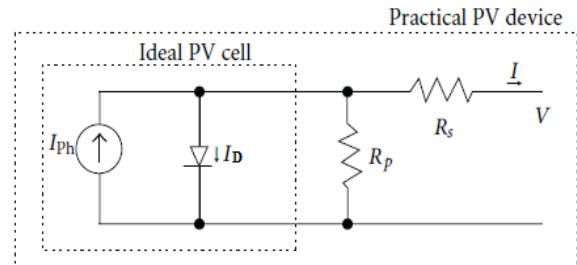


Figure 1. Equivalent circuit diagram of a solar PV cell

The diode is the one which determines the current-voltage characteristic of the cell. The output of the current source is directly proportional to the light falling on the cell. The open circuit voltage increases logarithmically according to the Shockley equation which describes the interdependent of current and voltage in a solar cell. An equation that represents I -V characteristics of a solar array is given by the following mathematical equation as

$$I = I_{ph} - I_s \left(e^{\frac{q(v+IR_s)}{mkT}} - 1 \right) - \left[\frac{V+IR_s}{R_p} \right] \text{----(1)}$$

Equation (1) is used in computer simulations to obtain the output characteristics of a solar cell. To simulate the selected PV array, a PV mathematical model having N_p cells in parallel and N_s cells in series is used according to the following equation (neglecting shunt resistance):

$$I = N_p I_{ph} - N_p I_s \left(e^{\frac{q(v+IR_s)}{(mkTN_s)}} - 1 \right) \text{----(2)}$$

Assuming N_p the above equation can be rewritten as:

$$I = I_{ph} - I_s \left(e^{\frac{q(v+IR_s)}{(mkTN_s)}} - 1 \right) \text{----(3)}$$

In particular, the cell reverse saturation current, I_s , varies with temperature according to the following equation as:

$$I_S = I_{S(T_1)} * \left(\frac{T}{T_1}\right)^3 * e^{\frac{-qV}{mK}} \left(\frac{1}{T} - \frac{1}{T_1}\right) \text{----- (4)}$$

$$I_{S(T_1)} = \frac{I_{SC(T_1)}}{(e^{qV_{OC}(T_1)/mKT_1} - 1)} \text{----- (5)}$$

The photo current I_{ph} , depends on the solar radiation (S) and the temperature (T) according to the following equation as:

$$I_{ph} = I_{ph(T_1)}(1 + K_0(T - T_1)) \text{----- (6)}$$

$$I_{ph(T_1)} = S * I_{SC(T_1, norm)} / S_{norm} \text{----- (7)}$$

Where $K_0 = (I_{S(T_2)} - I_{S(T_1)}) / (T_2 - T_1)$ ----- (8)

The series resistance of the cell is given as

$$R_S = \frac{dV}{dI_{VOC}} - \left(\frac{1}{X_V}\right) \text{----- (9)}$$

Where $X_V = I_{0(T_1)} * q / mKT_1 * (e^{qV_{OC}(T_1)/mKT_1} - 1)$ ----- (10)

The PV power, P, is then calculated as follows

$$P = N_P I_{ph} V - N_P I_S V \left(e^{\frac{q(V + I R_S)}{mKT N_S}} - 1 \right) = VI \text{----- (11)}$$

where

V - output voltage of PV module,

I - output current of PV module,

R_s - series resistance of cell (Ω)

R_{sh} - shunt resistance of cell (Ω)

q - electronic charge ($1.602 * 10^{-19}$ C),

I_{sc} - light-generated current,

K - Boltzman constant ($1.38 * 10^{-23}$ J/k),

T_k - temperature (K), n_s number of PV cells connected in series,

N_p - number of PV cells connected in parallel,

I_0 - reverse saturation current which depends on the ambient temperature

m - diode factor (usually between 1 and 2);

n_s : number of PV cell in series

n_p : number of PV cell in parallel

Using these fundamental equations and parameters from the data sheet, the PV model is developed and verified with the panel data sheet. The I-V characteristics of KC200GT for different irradiance levels at the cell temperature of 25°C and varying cell temperature for a constant irradiance level of 1000

W/m² as obtained from the simulation are shown in Figures 2(a) and (b), respectively. The similarities of the I-V curves for different conditions with the corresponding curves in the KC200GT panel datasheet prove the validity of the developed solar panel model. The parameters of the PV panel under study are shown in Table 1. The specifications of the selected PV panel Parameters at 1000 W/M² and 25° C is shown in Table 1

Table 1: Specifications of the PV panel

Model	Kyocera KC200GT
V_{MPP}	26.3 V
I_{MPP}	7.61 A
V_{SC}	32.90 V
I_{SC}	8.21 A
P_{MPP}	200.0 W

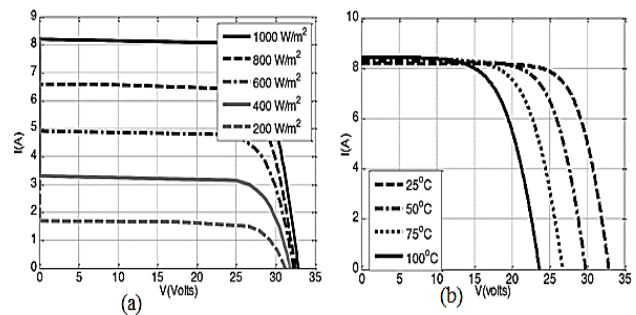


Figure 2. The I-V characteristics of Kyocera KC200GT from simulation with (a) varying irradiance at a cell temperature of 25° C (b) varying cell temperature at 1000W/m².

The PV system under study for the proposed V-f and P-Q control has 125 strings with each string having 4 series connected panels. The Maximum Power Point (MPP) for a single panel of KC200GT at 1000 W/m² and 25° C (STC) is 200 W. Hence, the maximum power of the PV generator at STC is 125 X 4 X 200 =100kW. But the MPP varies according to the change in irradiance level and cell temperature.

2. PV System Configuration And System Description

A. PV System Configuration

Figure 3 shows the PV system configuration for V-f and P-Q control with PV operating at MPP including the battery storage backup. It is a two-stage configuration where a DC-DC boost converter is used

for MPPT control. The system also considers a battery back-up in case of emergencies while maintaining the voltage and frequency of the micro-grid or while trying to supply the critical loads. A battery is connected in parallel to the PV to inject or absorb active power through a bidirectional DC-DC converter. When the battery is absorbing power, the converter operates in the buck mode and when battery is injecting power to the grid, it operates in the boost mode. The operation mode is maintained through the control signal provided to the converter switches. The PV system is connected to the grid through a coupling inductor L_C . The coupling inductor filters out the ripples in the PV output current. The connection point is called the point of common coupling (PCC) and the PCC voltage is denoted as $V_c(t)$. The rest of the system in Fig. 3 denotes the IEEE 13-bus distribution feeder which is simplified as a substation with the feeder equivalent impedance, $R+j\omega L_s$. The PV source is connected to the DC link of the inverter with a capacitor C_{dc} . The PV is the active power source, and the capacitor is the reactive power source of the PV system. According to the instantaneous power definitions for a balanced three-phase system consider $V_t(t)$ and $V_c(t)$ denote the instantaneous PCC voltage and the inverter output voltage (harmonics neglected) respectively, then the average power of the PV denoted as $P(t)$, the apparent power $S(t)$ and the average reactive power $Q(t)$ of the PV are as given by eqs.(12)-(14).

$$P(t) = \frac{2}{T} \int_{t-\frac{T}{2}}^t V_t(T) i_c(T) dt = \frac{V_t(t) V_c(t)}{\omega L_C} \sin \alpha \quad (12)$$

$$S(t) = V_t(t) I_c(t) = \frac{V_t(t)}{\omega L_C} \sqrt{V_t(t)^2 + V_c(t)^2 - 2V_t(t)V_c(t) \cos \alpha} \quad (13)$$

$$Q(t) = \sqrt{S^2(t) - P^2(t)} = \frac{V_t(t)}{\omega L_C} (V_c(t) \cos \alpha - V_t(t)) \quad (14)$$

Here, α is the phase angle of $V_c(t)$ relative to the PCC voltage. $P(t)$ and $Q(t)$ in (12) and (14) can be approximated by the first terms of the Taylor series if the angle α is small, as shown in (15) and (16):

$$P(t) \approx \frac{V_t(t) V_c(t)}{\omega L_C} \alpha \quad (15)$$

$$Q(t) \approx \frac{V_t(t)}{\omega L_C} (V_t(t) - V_c(t)) \quad (16)$$

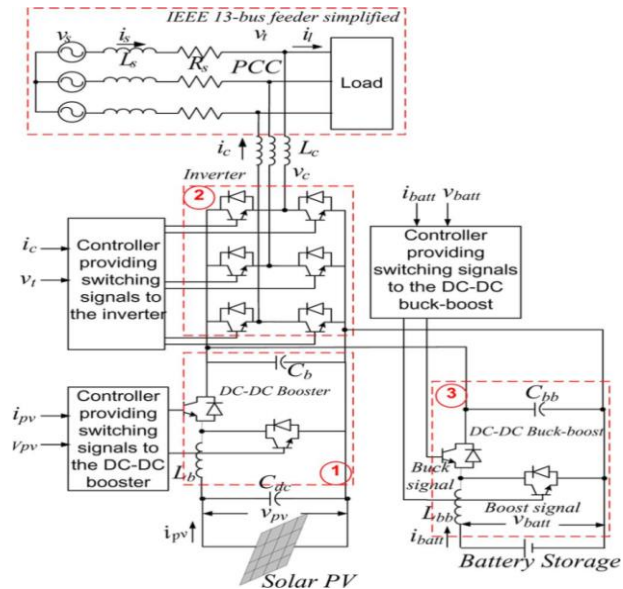


Figure 3. System configuration of V-f control with solar PV generator operating at MPPT with a battery storage system.

B. Battery Modeling

In this paper, the battery model is taken from the MATLAB SimPower Systems library with appropriate parameters which will be used for the proposed V-f and P-Q controls. It is assumed that the lead acid battery can be discharged up to SOC of 20% and can be charged up to SOC of 80%. The battery model is an analytical model with two equations representing the battery discharge and charge models. The battery discharge and charge model for a lead acid battery is given by equations. (17) and (18), respectively.

$$V_{Batt} = V_0 - R \cdot i - K \frac{Q}{q-it} (it + t^*) + Exp(t) \quad (17)$$

$$V_{Batt} = V_0 - R \cdot i - \left[K \frac{Q}{it-0.1Q} \right] i^* - \left[K \frac{Q}{Q-it} \right] \cdot it + Exp(t) \quad (18)$$

Where V_{Batt} is the battery voltage (V), V_0 is the battery constant voltage (V), K is polarization constant (V/Ah) or polarization resistance Q is battery capacity (Ah), $it = \int i dt$ battery charge (Ah), A is exponential zone amplitude (V), B is exponential zone time constant inverse (Ah), R is the internal resistance is battery current (A), i and is filtered current (A). The

size of the battery is selected to provide a maximum backup power to compensate for the PV generation in the case of a very small or no irradiance level. In this work, the MPP of PV generator at STC is 100 kW. Hence, the battery is chosen to provide of power for a maximum of 1 hour with an energy content of 100 kWh. The battery backup is considered for short duration applications like frequency control and supplying power to critical loads in the event of emergency situations One hour of battery backup is considered to be enough for other backup generators to take over the controls in the micro-grid emergency situations.

C. Description Of IEEE 13-Bus Distribution Feeder

The diagram of the IEEE 13-bus distribution test system is shown in Figure 4. It consists of a substation, 13 buses or nodes, 11 line sections, and 8 loads. The loads comprise of a combination of constant impedance, constant current, and constant power (ZIP) loads but most of them are constant power loads. The substation is at 115 kV and it is stepped down to 4.16 kV by a distribution transformer(T1). There is one more transformer (T2) which steps down 4.16 kV to 480 V. In the grid connected mode, the substation located at Bus 650 at 115 kV level is considered as a source. In an islanded micro-grid case, a diesel generator connected at the same bus supplies the micro-grid with a fixed amount of active power as referenced by the central controller (CC) of the micro-grid.

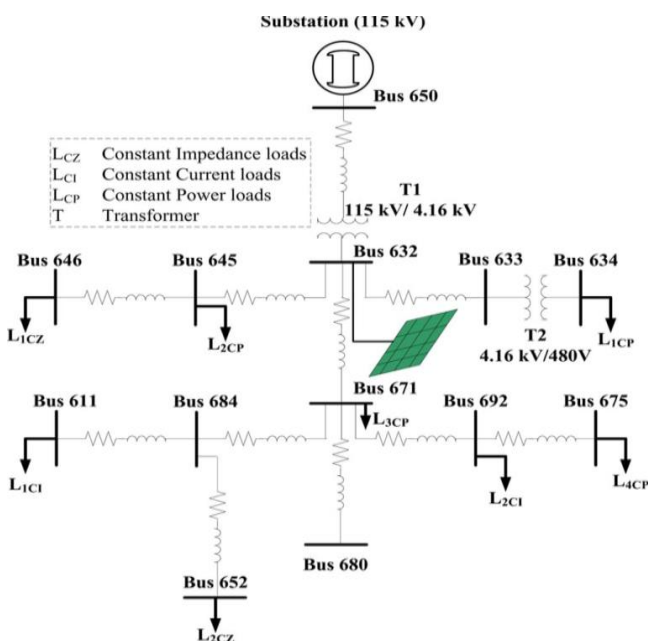


Figure 4. IEEE-13 bus distribution feeder.

3. MPPT and Battery Integrated V-F Control Method

The MPPT and battery integrated V-f control diagrams are shown in Figs. 5 and 6, respectively. The control comprises of one loop for MPPT control, two different loops for V-f control at the inverter side and another loop for battery power management. The loop 1 in Fig. 5 is a MPPT control. The actual PV power output, P_{PV} is compared with the MPP reference, P_{MPPref} from the lookup table 1 of irradiance versus MPP and this error is fed to a PI controller, PI_1 which outputs the duty cycle δ^* for the DC-DC boosters so that the array always operates at the referenced point by changing this duty cycle. The equation for this control loop is given by eq. (19). Here, K_{p1} and K_{i1} are the controller proportional and integral gains respectively for this control loop.

$$\delta^* = K_{p1} * (P_{MPPref} - P_{PV}) + K_{i1} * \int_0^t (P_{MPPref} - P_{PV}) dt \text{ -----(19)}$$

Another feedback PI controller is used for voltage control at AC side. As shown in the control diagram in Fig. 5 (loop 2), the PCC voltage is measured and the rms value of is $V_t(t)$ calculated. Then, the rms value $V_t(t)$ is compared to a voltage reference $V_t^*(t)$ which could be a voltage specified by the utility, and the error is fed to a PI controller. The inverter output voltage $V_C(t)^*$ is controlled so that it is inphase with the PCC voltage, and the magnitude of the inverter output voltage is controlled so that the PCC voltage is regulated at a given level $V_t^*(t)$. The control scheme can be specifically expressed as eq. (20).

$$V_{C1}^*(t) = V_t(t) \left[1 + K_{P2}(V_t^*(t) - V_t(t)) + K_{I2} \int_0^t ((V_t^*(t) - V_t(t)) dt) \right] \text{ ---- (20)}$$

Where K_{P2} and K_{I2} are the controller gains for this loop.

In (20), 1 has been added to the right-hand side such that when there is no injection from the PV generator, the PV output voltage is exactly the same as the terminal voltage. The frequency control is carried out by controlling the active power output at the inverter side as shown in the outermost loop3. The referenced micro-grid frequency of 60 Hz is compared with the

measured value and this error is fed to the PI controller P_{I3} that provides the phase shift contribution α_1^* which shifts the voltage waveform in timescale such that the active power injected will be enough to maintain the frequency at 60 Hz nominal value. The equation for this control is given by (21).

$$\alpha_1^* = K_{P3}(f_{ref} - f_{measured}) + K_{I3} \int_0^t (f_{ref} - f_{measured}) dt \text{ -----(21)}$$

There is another controller P_{I4} used in the same loop 3. This controller maintains active power balance between the AC and DC sides of the inverter. The reference signal for P_{I4} is obtained from the dynamically changing active power injection from the inverter at the AC side as determined by the output of P_{I3} . The measured AC side active power $P_{ACmeasured}$ is multiplied by a factor of 1.02 considering the efficiency of inverter as 98% such that the DC side active power is 102% of the AC side active power. The DC side active power is compared with this value of AC side power and the error is fed to P_{I4} to obtain the phase shift contribution from this loop as α_2^* . The equation for this control is given by (22).

$$\alpha_2^* = K_{P4}(1.02 * P_{AC} - P_{DC}) + K_{I4} \int_0^t (1.02 * P_{AC} - P_{DC}) dt \text{ -----(22)}$$

The phase shift contributions from DC and AC sides, α_1^* and α_2^* are then averaged as given by (23) to obtain the final phase shift, α^* of the voltage waveform, V_{C1*} which, then, generates the voltage reference signal V_{C*} for the inverter PWM.

$$\alpha^* = (\alpha_1^* + \alpha_2^*)/2 \text{ -----(23)}$$

Here, the reason behind considering phase shift contributions from both DC and AC side active power is to control the DC side voltage and achieve the desired value. By making α_1^* and α_2^* close in range through the controller gains, it can be assured that the active power at the DC and AC sides is balanced. This, coupled with the voltage control loop, assures that the DC side voltage is maintained at the value desired by the AC side voltage. The controls shown in the diagram of Figure 5 and described above are also integrated with the battery power control shown in Figure 6. The battery is incorporated in the PV system

configuration in order to supply or absorb active power and support the frequency control objective with the PV generator. If there is abundant solar power and the active power required for frequency control is less than PV MPP, then the battery will be charged. If there is not enough solar power available and if the active power required for frequency control is more than PVMPP, then the battery will supply the deficit power in order to maintain the micro-grid frequency at 60 Hz. Hence, the control method for the battery charge/discharge that depends on this requirement is developed as shown in Figure 6. It also shows the selection of charge and discharge modes which handle the battery SOC constraint and will be described later in the Part B of this section. In Figure 6, the reference power to the battery $P_{Battref}$ is generated dynamically by subtracting the inverter active power injection, $P_{inverter}$ from the power generated by PV, P_{PV} . The controller comprised of a PI controller, P_{I5} which receives the error signal obtained after subtracting the actual battery power, P_{Batt} from the battery reference, $P_{Battref}$. The signal obtained from P_{I5} is then compared with a triangular waveform of unity magnitude to generate the signal, S^* . This is similar to common Pulse Width Modulation (PWM) in inverter controls. K_{P5} and K_{I5} are the proportional and integral gains respectively. The equation for this control is given by (24).

$$S^* = K_{P5}(P_{Battref} - P_{Batt}) + K_{I5} \int_0^t (P_{Battref} - P_{Batt}) dt \text{(24)}$$

One more step is considered to differentiate the charging and discharging mode of the battery. This is undertaken by comparing P_{PV} with $P_{inverter}$. If $P_{PV} \geq P_{inverter}$, the battery is in charging mode, hence, the signal obtained from the PWM, S^* and the result of this comparison is passed through a logical AND to generate a switching signal which activates the Buck mode of the DC-DC converter. If the condition $P_{PV} > P_{inverter}$ is false, (i.e., $P_{PV} < P_{inverter}$), the opposite of this signal and S^* is passed through a logical AND to generate a switching signal which activates the Boost mode of the DC-DC converter. Hence, with this control logic, the converter is capable of operating in both directions and therefore, effectively charging and discharging the battery whenever required.

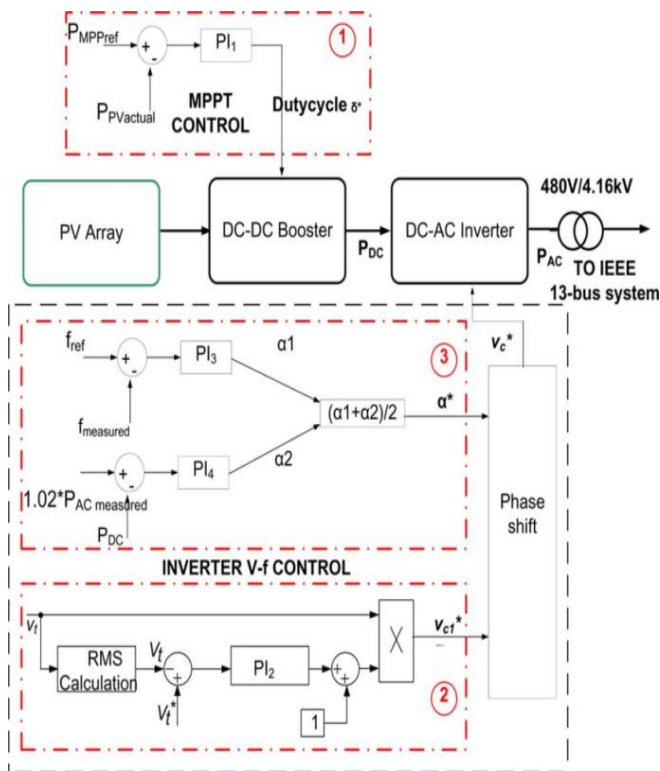


Figure 5. Integrated Solar PV MPPT and V-f control diagram.

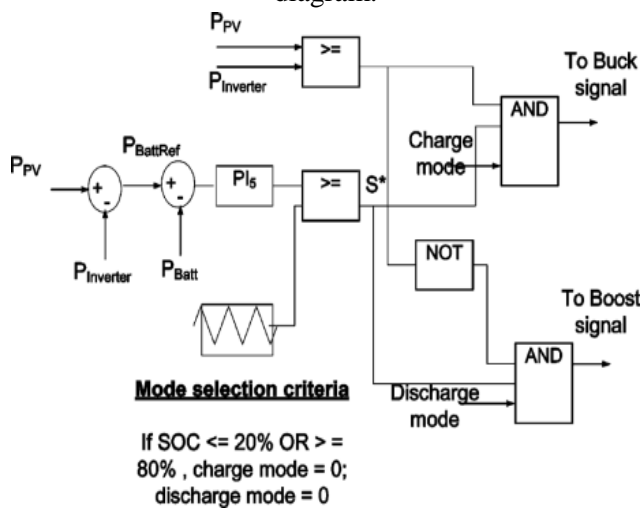


Figure 6. Battery power control diagram.

III. SIMULATION RESULTS AND DISCUSSIONS

This section presents the simulation results obtained with applications of the proposed control methods to the IEEE 13-bus distribution feeder. First, the results obtained from the coordinated V-f control are presented which is followed by the results from the coordinated P-Q control. In grid connected mode, the distribution feeder is considered to be supplied by a central generator with a substation at Bus 650 at 115 kV level and a PV generator at Bus 632. Hence, in an

islanded case, the distribution feeder is supplied by a diesel Generator and a PV connected at Buses 650 and 632, respectively. The Simulink diagram of the MPPT integrated with Battery of a Photovoltaic System for Micro Grid operation is shown in Figure 7.

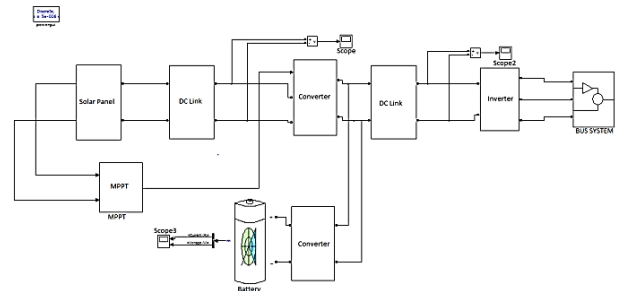


Figure 7. The Simulink diagram of the MPPT integrated with Battery of a Photovoltaic System for Micro Grid operation

For the demonstration of the V-f control algorithm, two different irradiance cases are considered: Case 1 with irradiance 1000 W/m² and Case 2 with 750 W/m². The PI controller gain parameters for Case 1 are given in Table 2. The controller gains should be adjusted slightly for the change in irradiance. While moving from the grid connected to micro-grid mode, the diesel generator is controlled to generate a fixed amount of active power according to the command from the central controller. The diesel generator produces a fixed amount of 1.25 MW throughout the simulation period as shown in Figure 8(a). It also shows the reactive power generated from the diesel generator. In the islanded mode, the active power generated by the diesel generator is not enough to fulfill the power demand of the micro-grid. Figures 8(b) and 8(c) shows the microgrid frequency which initially dips to a value of 57.8 Hz due to the load-generation imbalance. The frequency control from the PV generator starts at 0.1 sec which quickly regulates the frequency back to 60 Hz in 0.2sec. Figures 8(d) and 8(e) shows the plot of the PCC voltage in p.u. It can be observed that voltage is also quickly regulated at 1 p.u. after the control is started. Figures 8(f) and 8(g) shows the active and reactive power injection from the PV inverter which regulates the frequency and voltage of the micro-grid. The active power injection from the inverter, which is required to maintain the frequency at 60 Hz in both cases, is around 80 kW. However, there is a difference in the share of the PV generator and the battery energy

storage while providing the required 80 kW to the micro-grid. This is evident from Figure 8(h) which shows the active power from the PV, the battery, and the inverter, respectively, for both cases. In Case 1, solar irradiance is abundant at 1000 W/m² and hence, the PV generates the maximum power of 100 kW which is more than is required to maintain the micro-grid frequency. The surplus 20 kW is used to charge the battery. The negative sign in battery power means that it is a charging phase, i.e., the battery absorbs power is shown in Figure 8(h).

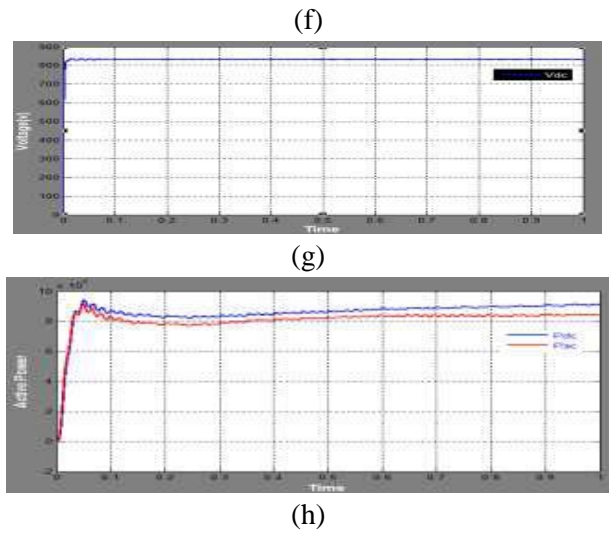
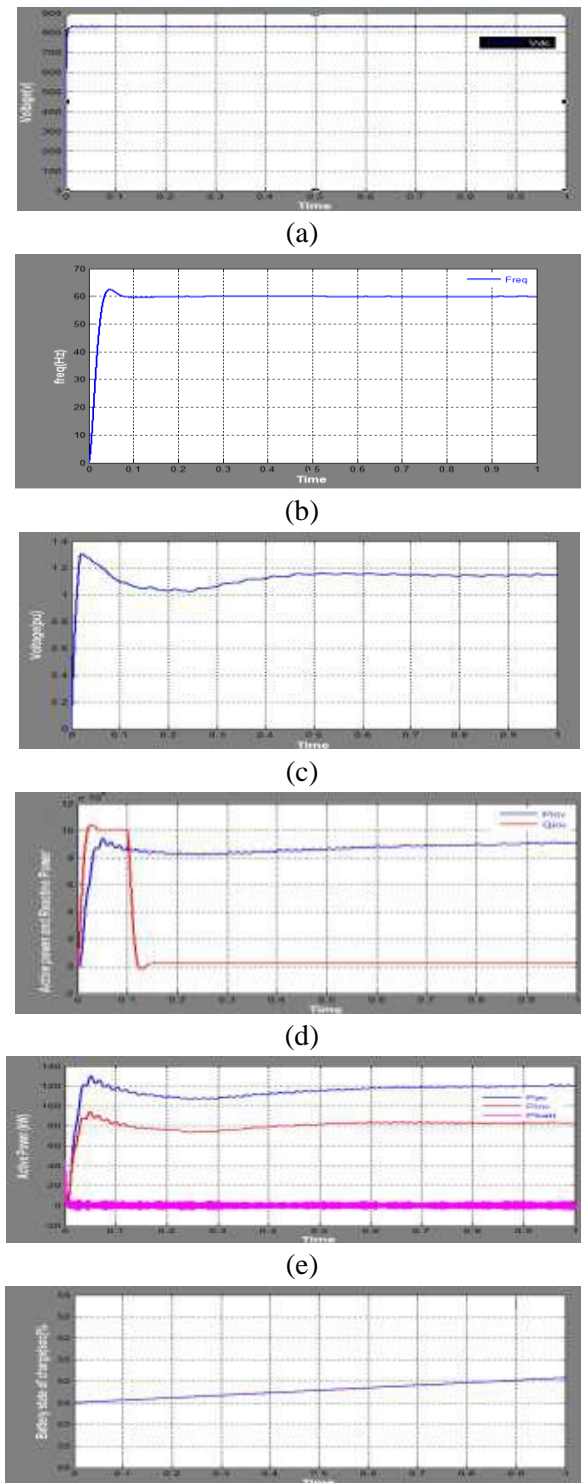


Figure 8. Results of coordinated V-f control with Solar PV including MPPT control and battery control.

IV. CONCLUSION

The contribution of this paper can be summarized as follows: This paper proposes and presents coordinated strategies of V-f control and P-Q control, respectively, for micro grids with PV generator and battery storage. In the control strategies, the PV generator is operated at MPP, and the battery storage acts as a buffer in order to inject and absorb deficit or surplus power by using the charge/discharge cycle of the battery. The paper contributes in demonstrating the control strategies with effective coordination between inverter V-f (or P-Q) control, MPPT control, and energy storage control. The proposed control strategy also provides a smooth transition of PV side PQ control in grid connected mode to V-f control in islanded mode. This is the most essential feature required in the modern micro-grid controllers. The proposed integrated and coordinated P-Q control algorithm can be effectively used in supplying some critical loads of a micro-grid with solar PV and battery. In the present methods, the control parameters are dependent upon the PV, battery, and external grid conditions and must be re-tuned with the changing conditions. This can be overcome by using an adaptive method to obtain these parameters dynamically based on the system conditions. The adaptive control methods could be a very useful and promising future direction of this work. The proposed control algorithms are also capable of handling the battery SOC constraint. An effective Seamless transformation of controls from V-f to constant active power and voltage control at the PV side and from constant active power control to

frequency control at the diesel generator is validated with satisfactory results. This feature helps the controller to adapt to the changing irradiance levels while considering the battery availability.

V. ACKNOWLEDGMENT

I express my thanks to the support given by management in completing my project. I also express my sincere gratitude & deep sense of respect to Dr. S.K Shrivastava, professor of the Electrical Department. I am thankful to the Research Head, teaching and non-teaching staff of Electrical department for their direct as well as indirect help in my project. I am elated to avail my selves to this opportunity to express my deep sense of gratitude to my parents.

VI. REFERENCES

- [1] H. Li, F. Li, Y. Xu, D. T. Rizy, and J. D. Kueck, "Adaptive voltage control with distributed energy resources: Algorithm, theoretical analysis, simulation and field test verification," *IEEE Trans. Power Syst.*, vol. 25, pp. 1638–1647, Aug. 2010.
- [2] L. D. Watson and J. W. Kimball, "Frequency regulation of a microgrid using solar power," in *Proc. 2011 IEEE APEC*, pp. 321–326.
- [3] M. G. Molina and P. E. Mercado, "Modeling and control of grid-connected photovoltaic energy conversion system Used as a dispersed generator," in *Proc. 2008 IEEE/PES Transm. Distrib. Conf. Expo.: Latin America*, pp. 1–8.
- [4] N. Kakimoto, S. Takayama, H. Satoh, and K. Nakamura, "Power modulation of photovoltaic generator for frequency Control of power system," *IEEE Trans. Energy Conv.*, vol. 24, pp. 943–949, 2009.
- [5] R. H. Lasseter, "MicroGrids," in *Proc. IEEE Power Engineering Society Winter Meeting, 2002*, vol. 1, pp. 305–308.
- [6] S. Chowdhury, S. P. Chowdhury, and P. Crossley, "Microgrids and Active Distribution Networks," 2009, *IET Renewable Energy Series 6*.
- [7] H. Saadat, *Power System Analysis*, 2nd ed. New York, NY, USA: Mc- Graw Hill, 2002.
- [8] J. A. P. Lopes, C. L. Moreira, and A. G. Madureira, "Defining control strategies for MicroGrids islanded operation," *IEEE Trans. Power Syst.*, vol. 21, pp. 916–924, 2006.
- [9] Y. Xu, F. Li, D. T. Rizy, and J. D. Kueck, "Active and nonactive power control with distributed energy resources," In *Proc 210. Tremblay and L. A. Dessaint*, "Experimental validation of a battery dynamic model for EV applications," *World Electric. 2008 40th North American Power Symp. NAPS'08*, pp. 1–7.
- [10] S. Adhikari et al., "Utility-side voltage and PQ control with inverterbased photovoltaic systems," in *Proc. 18th World Congr. IFAC, Milan, Italy, Aug. 28–Sep. 2 2011*, pp. 6110–6116.
- [11] H. Laaksonen, P. Saari, and R. Komulainen, "Voltage and frequency control of inverter based weak LV network Microgrid," presented at the *Int. Conf. Future Power Syst.*, Amsterdam, The Netherlands, Nov. 18, 2005.
- [12] J. C. Vasquez, R. A. Mastromauro, J. M. Guerrero, and M. Liserre, "Voltage support provided by a droop-controlled Multifunctional inverter," *IEEE Trans. Ind. Electron.*, vol. 56, pp. 4510–4519, 2009.
- [13] T. Ota, K. Mizuno, K. Yukita, H. Nakano, Y. Goto, and K. Ichiyanagi, "Study of load frequency control for a Microgrid," in *Proc. 2007 AUPEC Power Eng. Conf.*, pp. 1–6.
- [14] L. Xu, Z. Miao, and L. Fan, "Coordinated control of a solar battery system in amicrogrid," in *Proc. 2012 IEEE/PES Transm. Distrib. Conf. Expo. (T&D)*, pp. 1–7.
- [15] M. G. Villalva, J. R. Gazoli, and E. R. Filho, "Comprehensive approach to modeling and simulation of photovoltaic Arrays," *IEEE Trans. Power Electron.*, vol. 24, no. 5, pp. 1198–1208, 2009.
- [16] Y. Xu, H. Li, D. T. Rizy, F. Li, and J. D. Kueck, "Instantaneous active and nonactive power control of distributed Energy resources with a current limiter," in *Proc. IEEE Energy Conversion Congr. Expo. 2010*, pp. 3855–3861. *Vehicle J.*, vol. 3, 2009.
- [17] B. Awad, J. Wu, and N. Jenkins, "Control of distributed generation," *Electrotechn. Info.* (2008), vol. 125/12, pp. 409–414.
- [18] J. C. Vasquez, J. M. Guerrero, E. Gregorio, P. Rodriguez, R. Teodorescu, and F. Blaabjerg, "Adaptive droop control Applied to distributed generation inverters connected to the grid," in *Proc. 2008 IEEE ISIE*, pp. 2420–2425.
- [19] H. Bevrani and S. Shokoohi, "An intelligent droop control for simultaneous voltage and frequency regulation in Islanded microgrids," *IEEE Trans. Smart Grid*, vol. 4, no. 3, pp. 1505–1513, Sep. 2013.
- [20] J. C. Vasquez, J. M. Guerrero, M. Savaghebi, and R. Teodorescu, "Modelling, analysis and design of stationary Reference frame droop controlled parallel three-phase voltage source inverters," in *Proc. 2011 IEEE 8th ICPE & ECCE*, pp. 272–279.
- [21] T. L. Vandoorn, B. Meersman, J. D. M. De Kooning, and L. Vandevelde, "Analogy between conventional grid control And islanded microgrid control based on a global DC-link voltage droop," *IEEE Trans. Power Delivery*, vol. 27, no. 3, pp. 1405–1414, Jul. 2012
- [22] H. Li, F. Li, Y. Xu, D. T. Rizy, and S. Adhikari, "Autonomous and adaptive Voltage control using multiple distributed energy resources," *IEEE Trans. Power Syst.*, vol. 28, no. 2, pp. 718–730, May 2013.